

# Effects of fractal microreactor on mass transfer and reaction in methanol steam reforming<sup>#</sup>

Lianlian Xu, Haisheng Cui, Zhang Bai\*, Yunyi Han, Xiankun Huang, Yongxiao Tuo, Shuoshuo Wang

College of New Energy, China University of Petroleum (East China), Qingdao 266580, China

(Corresponding Author: [baizhang@upc.edu.cn](mailto:baizhang@upc.edu.cn))

## ABSTRACT

Hydrogen production by methanol steam reforming (MSR) is one of the promising solutions for mobile hydrogen sources, particularly in applications like proton exchange membrane fuel cells (PEMFCs) and hydrogen refueling stations. However, due to the endothermic characteristics of MSR, its hydrogen production efficiency is greatly affected by thermal management, such as temperature gradient and cold/hot spot. Considering portability and integrated applications, miniaturizing the reaction system to achieve efficient continuous hydrogen production is also a significant challenge. Using fractal geometry in engineering applications can produce larger surface area and lower mass devices. In order to improve the heat and mass transfer as well as the chemical reaction performance of the reforming system, this study uses the Sierpinski carpet model, which integrates four iterations of fractal geometry, into the design of the MSR microreactor. The fluid flow, heat transfer, and chemical reaction processes in MSR fractal microreactor are simulated by the finite element method. A comparison is made with a flat plate type reactor (0<sup>th</sup> order). The results indicate that the heat and mass transfer performance of the fractal microreactors is higher than that of the flat plate type reactor. Compared with the 0<sup>th</sup> order reactor, the 4<sup>th</sup> order fractal microreactor can effectively improve the utilization efficiency of H by about 8.33% and improve the H<sub>2</sub> production rate by 7.91%. In addition, a higher steam/CH<sub>3</sub>OH (S/C) mole ratio results in a higher H utilization efficiency, the relative concentration of CO at the outlet, and the H<sub>2</sub> production rate, while a higher reforming temperature results in a lower H<sub>2</sub> production rate. This study can provide a theoretical basis and technical support for the industrial application of microreactors in mobile hydrogen production and fuel cells.

**Keywords:** methanol steam reforming, hydrogen production, microreactor, fractal

## NONMENCLATURE

### *Symbols*

|           |  |
|-----------|--|
| $A$       | Pre-exponential factor                         |
| $E_a$     | Activation energy, kJ/mol                      |
| $f$       | The friction coefficient                       |
| $\bar{h}$ | The average heat transfer coefficient, W/(m·K) |
| $Nu$      | Nusselt number                                 |
| $\varphi$ | Relative concentration, ppm                    |
| $\eta$    | Gas production rate, mmol/h                    |
| $\xi$     | Thermal-hydraulic performance parameter        |

## 1. INTRODUCTION

Vigorously developing hydrogen energy technology and industry is an important initiative to promote clean and low-carbon transformation of energy structure, it is estimated that hydrogen energy will account for about 18% of global energy demand in 2050 [1]. However, hydrogen supply restricts the further development of mobile hydrogen sources, particularly in applications like proton exchange membrane fuel cells (PEMFCs) and hydrogen refueling stations. On-site hydrogen production by reforming hydrocarbons (such as methane, DME, methanol, propane, etc.) is a feasible method to solve this limitation [2]. Methanol steam reforming (MSR) for hydrogen production is more beneficial among these methods due to its low reaction temperature, moderate conditions, and low energy consumption. Whereas it is a big challenge for MSR to achieve efficient continuous hydrogen production in mobile scenarios and miniaturize the reaction system. Fortunately, microreactor technology offers a good solution [3].

At present, several microreactor structures for hydrogen production by MSR, including parallel, serpentine, U-shaped, spiral, honeycomb, and microarray, have been studied experimentally and by numerical simulation. These studies have shown that the design of reactor structures plays an essential role in the fluid flow, heat transfer, and chemical reaction behavior of microreactors [4, 5]. Compared with traditional

<sup>#</sup> This is a paper for the 10th Applied Energy Symposium: Low Carbon Cities & Urban Energy Systems (CUE2024), May. 11-12, 2024, Shenzhen, China.

European geometry, the fractal structures are widely adopted to optimize heat and mass transfer in practical engineering by producing devices with a larger surface area and lower weight and have been involved in optimizing heat radiators, fuel cells, and chemical reactor design [6].

Yuan et al. [7] proposed a tubular microreactor with Cantor structure by introducing fractal theory and found that increased fractal dimension could promote the mixing of reactants and make the distribution of substance concentration in the channel more uniform. Yin et al. [8] evaluated the performance of the tree-shaped fractal channel under different working conditions, indicating that the fractal network is conducive to improving heat and mass transfer. Huang et al. [9] found that fractal design improved methanol conversion and reduced carbon monoxide concentration compared with parallel channels. Notably, the fractal unit of the Sierpinski carpet is the most widely used model in fractal theory, and its structure is similar to the topology of metal foam. Compared with the tree-like fractals, it has a larger surface area and more straightforward structure. In addition, it can provide more efficient heat and mass transfer channels in both horizontal and vertical directions. However, the design of the methanol microreformer does not propose the fractal element structure of the Sierpinski carpet. Sierpinski carpets have long been found to be more effective in natural and mixed convection than traditional large-surface ribbing columns and fins [10]. Calamas et al. [11] found that the Sierpinski carpet increased the mixing effect while slowing down the flow rate of the working fluid. With fractal iteration, the carpet efficiency per unit mass increased despite the decrease in the carpet efficiency.

The reasonable structure design of the reformer has a significant impact on hydrogen production performance. However, heat and mass transfer in the flow channel of the Sierpinski carpet structure with self-similar fractal characteristics is a complicated process. Therefore, the heat and mass transfer process of the reactor with different orders is evaluated and compared with that of the flat plate type reactor. The principle of MSR optimization with fractal structure is described, and the reason for the difference in steam/CH<sub>3</sub>OH (S/C) mole ratio and reforming temperature in the hydrogen production process of fractal microreactor is discussed.

## 2. METHODOLOGY

### 2.1 Fractal microreactor model

A fractal microreactor with a Sierpinski carpet structure for MSR is designed to reduce the parasitic

losses and improve the compact structure, considering the complex manifold distribution inside the reactor. Fig. 1 shows a diagonal Z-type buffer basin designed for the microreactor with a deflection of 45° and a length of  $L_0=10$  mm is designed for the microreactor. The blue shaded area in Fig. 1 is the fluid domain, the reactor wall thickness is 1 mm, and the size of the reaction zone is  $L_r*W_r=50*50$  mm. The reactor adopts the Sierpinski carpet structure shown in Fig. 2, in order to enhance the required efficient reforming environment and promote the hydrogen production rate. In each iteration, the Sierpinski carpet first divides the square into nine smaller squares in a 3 by 3 grid and then removes the smaller square in the middle. In this study, the fractal microreactor is constructed using the first 4 iterations of the Sierpinski carpet, and the fractal dimension of the Sierpinski carpet can be determined as  $D_f=\ln 7/\ln 3=1.77124$ . In order to prove the advantages of fractal microreactors, a flat plate type reactor (0<sup>th</sup> order) is constructed. Considering the precise self-similarity and micro-scale characteristics of the Sierpinski carpet and the reduction of calculation cost, the central cross-section of the fractal microreactor is used as the numerical model in the simulation.

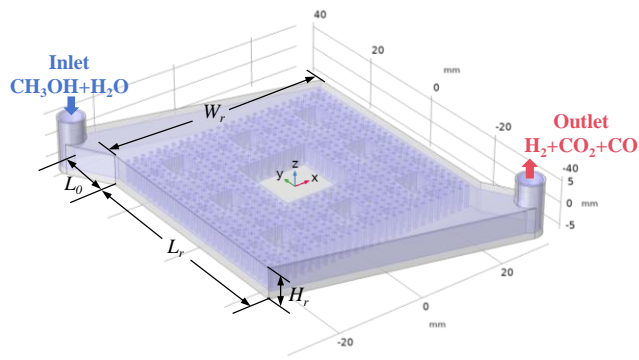


Fig. 1 Physical model of the fractal microreactor

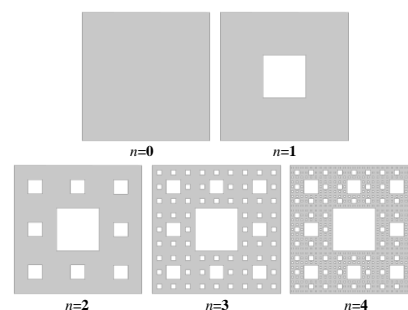
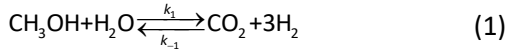


Fig. 2 Iteration of the Sierpinski carpet

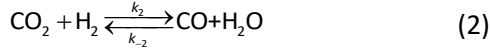
### 2.2 Methanol steam reforming

In this study, the CuO/ZnO/Al<sub>2</sub>O<sub>3</sub> commercial catalyst (SCST-401) is uniformly deposited on the channel wall, and the reaction occurred only on the wall. The Langmuir-Hinshelwood kinetic model proposed by Purnama et al. [12] is adopted to characterize the reaction on the catalyst surface:

Steam reforming, SR:



Reversed water gas shift, rWGS:



Purnama et al. [12] also gave the kinetic equation (3) and (4) for CuO/ZnO/Al<sub>2</sub>O<sub>3</sub> catalyst at the standard pressure and temperature range of 503.15-573.15 K through experiments, and obtained the rate constant  $k$ , activation energy  $E_a$  and pre-exponential factor  $A$  of the two reactions (Table 1).

$$r_{\text{SR}} = k_1 P_{\text{CH}_3\text{OH}}^{0.6} P_{\text{H}_2\text{O}}^{0.4} \quad (3)$$

$$r_{\text{rWGS}} = k_2 P_{\text{CO}_2} P_{\text{H}_2} - k_{-2} P_{\text{H}_2\text{O}} P_{\text{CO}} \quad (4)$$

In the reaction rate formula,  $k_1$  and  $k_2$  are the forward reaction rate constants,  $k_{-2}$  is the backward reaction rate constants, and  $P$  is the partial pressure of each component.

Table 1 Reaction rate constant, activation energy, and pre-exponential factor of MSR

|                   | SR                              | rWGS                               | WGS                             |
|-------------------|---------------------------------|------------------------------------|---------------------------------|
|                   | $k_1$ (1/(s·g <sub>cat</sub> )) | $k_{-2}$ (1/(s·g <sub>cat</sub> )) | $k_2$ (1/(s·g <sub>cat</sub> )) |
| $T$ (K)           |                                 |                                    |                                 |
| 503.15            | 2.5                             | 0.07                               | 7.8                             |
| 523.15            | 5.2                             | 0.19                               | 14.6                            |
| 543.15            | 9.8                             | 0.57                               | 31.7                            |
| 573.15            | 22.3                            | 1.59                               | 54.8                            |
| $E_a$<br>(kJ/mol) | 76                              | 108                                | 67                              |
| $A$               | $8.8 \times 10^8$               | $6.5 \times 10^9$                  | $4.0 \times 10^7$               |

### 2.3 Governing equation

In order to simplify the numerical analysis, the following assumptions are adopted: (1) All substances are in the gas phase, and methanol and water have been vaporized into the gas phase before entering the reactor. (2) The flow is considered to be a weakly compressible steady laminar flow. (3) The porosity and permeability of the catalyst are considered to be uniform. (4) Chemical reactions occur only in the catalyst reaction area. (5) Gravity and other forms of physical force are negligible. (6) Ignore thermal radiation. Based on these assumptions, the characteristics of the MSR in the microreactors can be obtained by solving the following equations:

$$\nabla \cdot (\rho \mathbf{u}) = 0 \quad (5-1)$$

$$\rho (\mathbf{u} \cdot \nabla) \mathbf{u} = \nabla \cdot [-p\mathbf{I} + \mathbf{K}] + \mathbf{M} \quad (5-2)$$

$$d_z \rho C_p \mathbf{u} \cdot \nabla T_s + \nabla \cdot \mathbf{q} = d_z Q + q_0 + d_z Q_p + d_z Q_{vd} \quad (5-3)$$

$$\nabla \cdot (-D_i \nabla c_i) + \mathbf{u} \cdot \nabla c_i = R_i \quad (5-4)$$

where  $\rho$  is the density,  $p$  is the pressure,  $c$  is the concentration,  $R$  is the reaction rate,  $d_z$  is the thickness of the domain in the out-of-plane direction,  $C_p$  is Specific heat capacity at constant pressure,  $T_s$  is the solid temperature,  $D$  is the diffusion coefficient,  $\mathbf{u}$  is the velocity vector,  $\mathbf{K}$  is the viscous stress tensor,  $\mathbf{M}$  is the volume force vector,  $\mathbf{q}$ ,  $q_0$ ,  $Q$ ,  $Q_p$ , and  $Q_{vd}$ , is conductive heat flux, inward heat flux, heat source, pressure work and viscous dissipation, respectively.  $i$  represents the substance composition.

### 2.4 Numerical methods and verification

The boundary conditions of the numerical simulation of the model are as follows:

(1) Inlet: A vapor mixture of methanol and water is preheated to 523.15 K and fed into the reactor at a volume flow rate of  $q_{\text{in}} = 0.01$  ml/min;

(2) Outlet: A zero outlet pressure is used as the reference pressure;

(3) Wall: The reactor solid material is 316L, and the wall is set up as a thermostatic no-slip wall at 523.15 K. All other surfaces are adiabatic no-slip walls.

The finite element program COMSOL and PARDISO parallel sparse direct solver are adopted to calculate MSR. Five grids of different densities are divided on the 4<sup>th</sup> order fractal microreactor. The grid independence is evaluated by the distribution of pressure and methanol mole fraction near the central axis of the microreactor, and the results are shown in Fig. 3. The pressure fluctuation is due to the confusion of the flow pattern caused by the fluid hitting the wall. The slowdown in the  $m_{\text{CH}_3\text{OH}}$  decline is due to the completion of the MSR of most of the reactants at the entrance. It can be seen that mesh refinement results in pressure differentials under 0.62% and methanol molar fraction changes below 1.00%.

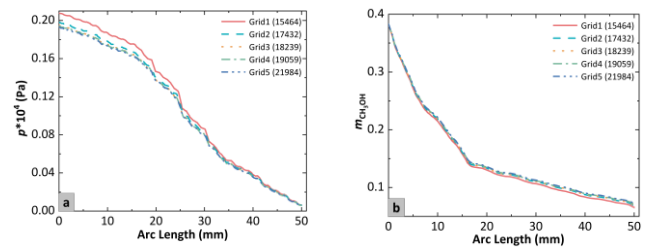


Fig. 3 (a) The pressure distribution and (b) the methanol molar fraction distribution near the central axis of the fractal microreactor with different meshing strategies

In order to verify the proposed model, five operating conditions in the experimental data of Zhang et al. [4] are selected as boundary conditions. From the changes of methanol conversion in the microreactor under different reaction solution flow rates (Fig. 4), it can be seen that the simulated value of the simulation result curve obtained by

this method is in a good agreement with the experimental value, with an average deviation of only 2.40%.

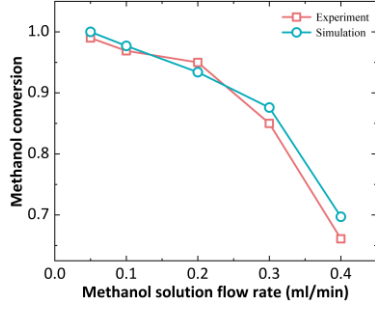


Fig. 4 Model verification: methanol conversion at different methanol solution flow rates

In order to evaluate the performance of the MSR microreactors, methanol conversion, hydrogen selectivity, relative concentration of CO, and hydrogen production rate are important factors. The combined performance of methanol conversion and hydrogen selectivity can be evaluated using the H utilization efficiency. The calculation formulas [13] are as follows:

$$\text{H utilization efficiency, } X(\text{H}) = \frac{2F_{\text{H}_2, \text{out}}}{4F_{\text{CH}_3\text{OH}, \text{in}} + 2F_{\text{H}_2\text{O}, \text{in}}} \times 100\% \quad (6)$$

$$\text{Relative concentration of CO, } \varphi_{\text{CO}} = \frac{m_{\text{CO}}}{m_{\text{H}_2} + m_{\text{CO}_2} + m_{\text{CO}}} \times 100\% \quad (7)$$

$$\text{H}_2 \text{ production rate, } \eta_{\text{H}_2} = F_{\text{out}} \cdot C_{\text{H}_2} \quad (8)$$

where,  $F_{\text{CH}_3\text{OH}, \text{in}}$  and  $F_{\text{H}_2\text{O}, \text{in}}$  are the molar feed flow rate of methanol and water in the reactant,  $F_{\text{H}_2\text{O}, \text{out}}$  is the molar flow rate of hydrogen in the gas production, and  $m_i$  is the molar fraction of each species in the gas production.

### 3. RESULTS AND DISCUSSION

#### 3.1 Effectiveness of the fractal microreactors

As the main reaction site of the MSR, the heat and mass transfer performance of the microreactors determines the hydrogen production performance of the methanol reformer. The fluid flow and heat transfer performance of five different types of microreactors are revealed by numerical simulation. Based on the friction coefficient and Nusselt number, thermal-hydraulic performance parameter [6] are introduced to evaluate the influence of iterative orders of the fractal microreactor on the heat and mass transfer performance, as shown in Fig. 5 and Fig. 6 ( $S/C=1.3$ , reforming temperature  $T=523.15$  K,  $q_{\text{in}}=0.01$  ml/min).

$$\text{friction coefficient, } f = \frac{d_0 \cdot \Delta p}{L \rho u^2} \quad (9)$$

$$\text{Nusselt number, } Nu = \frac{\bar{h} \cdot d_0}{\lambda} = \frac{Q \cdot d_0}{(T_s - T_f) \lambda} \quad (10)$$

$$\text{thermal-hydraulic performance parameter, } \xi = \frac{\bar{h}}{\Delta p} \quad (11)$$

where,  $\Delta p$  is the pressure drop between the inlet and outlet of the microreactor,  $L$  is the distance between the inlet and outlet of the microreactor,  $u$  is the average velocity, the inlet diameter  $d_0$  is selected as the characteristic length,  $\bar{h}$  is the average heat transfer coefficient,  $\lambda$  is the thermal coefficient, and  $T_f$  is the fluid temperature.

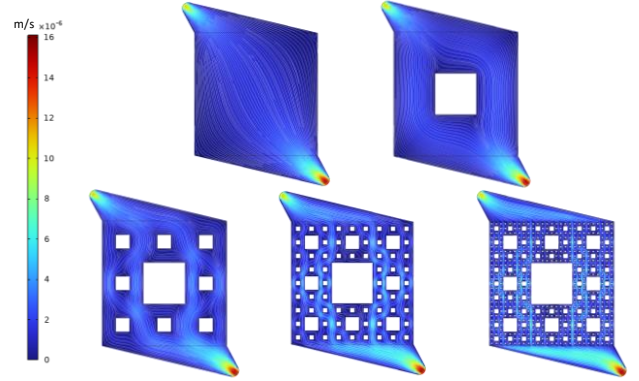


Fig. 5 Flow field of vapor mixture in the fractal microreactors

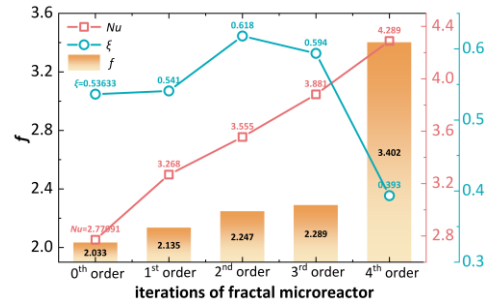


Fig. 6 The heat and mass transfer performance of the microreactors

The flow velocity distribution can provide basic information to understand the pressure-driven fluid flow in the microreactor. As shown in Fig. 5, the volume flow rate is  $q_{\text{in}}=0.01$  ml/min, the fractal microreactor presents the mixing and separation of flow lines at the rib columns of the Sierpinski carpet. Due to the presence of the rib column, the flow pattern (white line) changes significantly. It can be seen from the figure that the flow rate of the fractal microreactor increases with the increase of the iteration order. The 4<sup>th</sup> order fractal microreactor has the most uniform flow field distribution.

The Nusselt number increases with increasing fractal iterations at an average rate of 11.59% of the step size. However, the  $f$  of the 4<sup>th</sup> order is significantly increased by about 1.37 compared with  $f$  of the 0<sup>th</sup> order (Fig. 6). This is due to an increase in the number of rib columns in the 4<sup>th</sup> order Sierpinski carpet, which amplifies the micro-scale influence of fluid area. In particular, the fluid flow pattern at the entrance is destroyed to a large extent, which accords with the characteristic that the continuous iteration of the fractal means that the structure tends to

converge. It is also due to the increase of the inlet pressure that the  $\xi$  of the 4<sup>th</sup> order decreases. However, fractal iteration leads to more wall impact in the basin, which enhances the convective heat transfer. In summary, the first 3 iterations of the fractal microreactor can enhance the heat transfer capacity and keep  $f$  basically stable, which seems to be in line with expectations.

### 3.2 Distribution of mole fraction in fractal microreactors

In the study of chemical reaction kinetics, the change of molar fraction of gas components before and after the reforming reaction is often used to characterize the equilibrium property of the reaction. Fig. 7 depicts the mole fraction distribution of different species ( $i=\text{CH}_3\text{OH}$ ,  $\text{H}_2\text{O}$ ,  $\text{H}_2$ ,  $\text{CO}_2$ ,  $\text{CO}$ ) in the 4<sup>th</sup> order fractal microreactor under the same conditions as in Fig. 6. Along the flow direction of the reaction vapor, the molar fractions of  $\text{CH}_3\text{OH}$  and  $\text{H}_2\text{O}$  decrease, while the molar fractions of  $\text{H}_2$ ,  $\text{CO}_2$ , and  $\text{CO}$  increase. The decrease of  $m_{\text{CH}_3\text{OH}}$  and  $m_{\text{H}_2\text{O}}$  at the entrance of the reaction area are more pronounced, which is because the accumulation of liquid in the Z-type buffer basin promotes the SR reaction rate. The SR reaction at the entrance is dominant occurrence. In addition, the ratio of  $\text{H}_2$  and  $\text{CO}_2$  molar fractions is not precisely equal to 3, because the rWGS reaction is considered in the MSR.

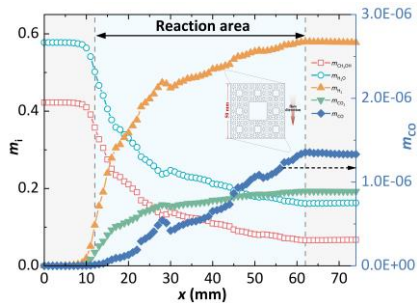


Fig. 7 The molar fractions distribution of different species along the vapor flow

### 3.3 Effect of steam/ $\text{CH}_3\text{OH}$ mole ratio and reforming temperature on the performance of MSR

In general, the steam/ $\text{CH}_3\text{OH}$  mole ratio and reforming temperature have a significant effect on the hydrogen production efficiency. Fig. 8 illustrates the impact of  $S/C$  on  $X(\text{H})$ ,  $\varphi_{\text{CO}}$  and  $\eta_{\text{H}_2}$  at a reforming temperature of 523.15 K and  $q_{\text{in}}=0.01$  ml/min. It is found that with an increase in  $S/C$ ,  $X(\text{H})$  and  $\eta_{\text{H}_2}$  increase by 8.33% and 7.91%, respectively. This can be attributed to the fact that both SR and rWGS develop further in the direction of  $\text{H}_2$  generation as the concentration of  $\text{H}_2\text{O}$  in the feed vapor increases. When  $S/C$  increases from 1 to 2,  $\varphi_{\text{CO}}$  decreases and then increases. As the WGS reaction proceeds, more  $\text{CO}$  is produced as  $\text{CO}_2$ . However, the increase of  $S/C$  also promotes the

generation of large amounts of  $\text{CO}_2$  in the SR reaction, thus enhancing the reverse reaction of WGS.

On the other hand, the 4<sup>th</sup> order fractal microreactor significantly extends the reaction time of reactants in the reaction area and improves the  $X(\text{H})$  in the reactor. At the same time, the  $\eta_{\text{H}_2}$  also increased significantly with the 4<sup>th</sup> order, but the relative concentration of  $\text{CO}$  also increased. Therefore, in practical applications, high  $S/C$  is a better choice. However, it should be noted that a higher proportion of water means that more energy is required for feed preheating, and considering that the relative concentration of  $\text{CO}$  will affect the energy utilization, such as PEMFC, it is more appropriate to choose  $S/C=1.3$ .

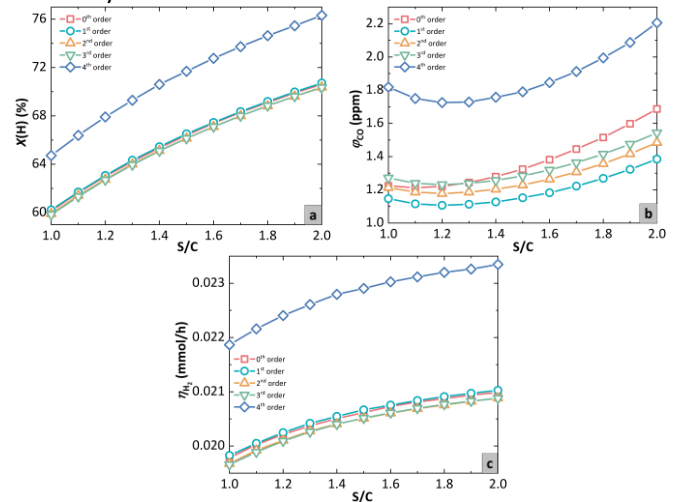


Fig. 8 Influence of  $S/C$  on (a)  $X(\text{H})$ , (b)  $\varphi_{\text{CO}}$ , and (c)  $\eta_{\text{H}_2}$  at  $q_{\text{in}}=0.01$  ml/min and  $T=523.15$  K

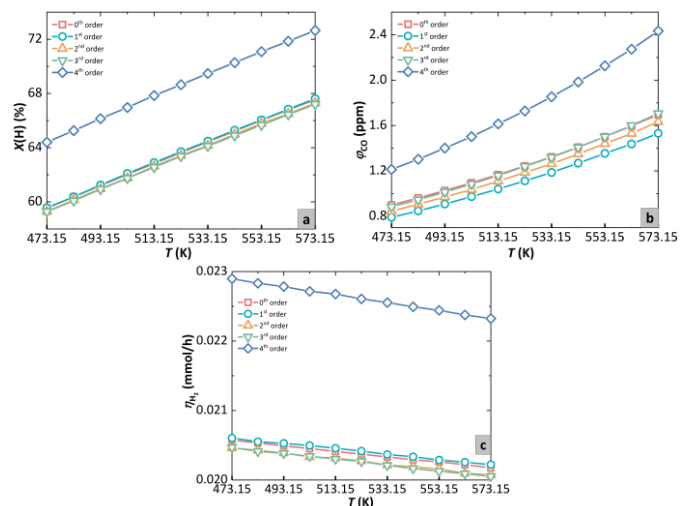


Fig. 9 Influence of  $T$  on (a)  $X(\text{H})$ , (b)  $\varphi_{\text{CO}}$ , and (c)  $\eta_{\text{H}_2}$  at  $q_{\text{in}}=0.01$  ml/min and  $S/C=1.3$

It is found that a higher  $X(\text{H})$  can be obtained at a higher temperature. MSR is an endothermic reaction, and a higher  $T$  can increase catalyst activity, speed up the reaction rate, and convert more methanol to  $\text{H}_2$ . On the other hand, an increase in  $T$  can improve the SR reaction.

However, the rWGS reaction is also activated, thus consuming more CO<sub>2</sub> and H<sub>2</sub> to produce CO, as shown in Fig. 9. Compared with the effect of S/C on the hydrogen production performance of methanol steam reforming, the effect of *T* seems more significant. Because the high temperature can easily lead to premature catalyst deactivation. In addition, higher *T* requires more heat supply, which may reduce system efficiency. Therefore, *T*=523.15 K is appropriate for high *X*(H) and low relative concentrations of CO.

#### 4. CONCLUSIONS

Effective microreactor design is the critical factor in ensuring the hydrogen production efficiency of methanol steam reforming. In this study, a self-similar fractal structure of the Sierpinski carpet is designed. The effect of fractal iterations on the flow and heat transfer performance of the MSR is investigated at the inlet temperature of 523.15 K and volume flow rate of 0.01ml/min. The results show that:

(1) The Sierpinski carpet structure increases the convective heat transfer capacity of the microreactors. Compared with the flat plate type microreactor, the Nusselt number increases with the fractal iteration at an average step size of 11.59%. And the first 3 iterations can keep the friction coefficient stable, providing a more uniform flow environment for the reaction.

(2) Based on the reaction rate model of MSR, SR reaction dominates in the microreactor, especially at the inlet. However, at high *T* and high S/C, rWGS will be activated with the SR reaction, which leads to the increase of CO mole fraction.

(3) The fractal structure prolongs the contact time between the reactants and the catalyst. With the increase of S/C, the H utilization rate and H<sub>2</sub> production rate of the 4<sup>th</sup> order fractal microreactor increased by 8.33% and 7.91%, respectively, compared with the 0<sup>th</sup> order fractal microreactor. With the increase of *T*, the CO concentration further increases.

#### ACKNOWLEDGEMENT

The authors appreciate the financial support provided by the National Natural Science Foundation of China (No. 52176030), Shandong Provincial Natural Science Foundation of China (ZR2022YQ58), Taishan Scholars Program of Shandong Province (No. tsqn202312115).

#### REFERENCE

[1] Yusaf T, Laimon M, Alrefae W, Kadirgama K, Dhahad H A, Ramasamy D, Kamarulzaman M K, Yousif B. Hydrogen energy demand growth prediction and assessment (2021–2050) using a system thinking and

system dynamics approach. *Applied Sciences*. 2022;12:781.

[2] Chen S, Pei C, Gong J. Insights into interface engineering in steam reforming reactions for hydrogen production. *Energy & Environmental Science*. 2019;12:3473-3495.

[3] Mei D, Qiu X, Liu H, Wu Q, Yu S, Xu L, Zuo T, Wang Y. Progress on methanol reforming technologies for highly efficient hydrogen production and applications. *International Journal of Hydrogen Energy*. 2022;47:35757-35777.

[4] Zhang S, Zhang Y, Chen J, Zhang X, Liu X. High yields of hydrogen production from methanol steam reforming with a cross-U type reactor. *Plos one*. 2017;12:e0187802.

[5] Yadav D, Lu X, Vishwakarma C B, Jing D. Advancements in microreactor technology for hydrogen production via steam reforming: A comprehensive review of experimental studies. *Journal of Power Sources*. 2023;585:233621.

[6] Xu L, Xu Y, Gu H, Qiu S, Mujumdar A S, Xu P. Thermal-hydraulic performance of flat-plate microchannel with fractal tree-like structure and self-affine rough wall. *Engineering Applications of Computational Fluid Mechanics*. 2023;17:e2153174.

[7] Yuan Z, Chen X. NO reduction mechanism in microreactor with cantor fractal structure. *Journal of Chemical Technology & Biotechnology*. 2022;97:2889-2897.

[8] Yin B, Chen Z, Xu S, Zhang S, Dong F. Effects of fractal network channel on heat and mass transfer in methanol steam reforming. *International Journal of Hydrogen Energy*. 2022;47:34810-34824.

[9] Huang Y, Chen D, Zheng Y, Liu X. Performance investigation and optimization of latent heat storage exchangers with sandwiched tree-channels. *International Journal of Heat and Mass Transfer*. 2022;183:122161.

[10] Zhang C, Wu L, Chen Y. Study on solidification of phase change material in fractal porous metal foam. *Fractals*. 2015;23:1540003.

[11] Calamas D M, Dannelley D G, Keten G H. Experimental effectiveness of Sierpinski carpet fractal fins in a natural convection environment. *Journal of Heat Transfer*. 2017;139:092501.

[12] Purnama H, Ressler T, Jentoft R E, Soerijanto H, Schlögl R, Schomäcker R. CO formation/selectivity for steam reforming of methanol with a commercial CuO/ZnO/Al<sub>2</sub>O<sub>3</sub> catalyst. *Applied Catalysis A: General*. 2004;259:83-94.

[13] Lu W, Zhang R, Toan S, Xu R, Zhou F, Sun Z, Sun Z. Microchannel structure design for hydrogen supply from methanol steam reforming. *Chemical Engineering Journal*. 2022;429:132286.